2E2-5

Beam Focused Slot Antenna for Microchip Implants

Yuji Tanabe, Hang Wong, Sanghoek Kim, John S. Ho and Ada S. Y. Poon
Department of Electrical Engineering, Stanford University
Room 237, Packard Electrical Engineering Building
350 Serra Mall Stanford, CA 94035
Email: ytanabe@stanford.edu

1. Introduction

Wireless powering of implantable medical devices such as pacemakers, cardiac defibrillators and other devices for post-surgery monitoring and drug delivery enables device miniaturization and obviates risks associated with lead wires and battery replacement. Traditionally, inductively-coupled coils have been considered the primary candidate for power transfer since they operate at frequencies sufficiently low to ignore losses in tissue [1]. Recently, however, it was shown that the optimal frequency for wireless power transfer to a miniature implant is in the low-GHz range despite increased tissue absorption [2]. At low-GHz frequencies, the power transfer efficiency was significantly improved by considering transmitter structures more complex than the coil. In particular, the optimal transmitter was found to exhibit beam focusing, which invokes constructive and destructive interference to maximize the fields at the receiver while minimizing heating in tissue. The optimal transmitter, however, was derived in terms of a surface current distribution and was not physically realized [3], [4].

This paper proposes a beam focused transmitter implemented by four curved slot antennas and a 4-port feed network that synthesizes the optimal current distribution. We first examine the dominant current found in [4] for a receiver modeled as a magnetic dipole (i.e. small coil) and obtain a simplified current distribution. The simplified distribution is realized by a pair of slot antennas which is used to design an array that is robust to the horizontal orientation of the receiver coil.

2. Simplified Optimal Current Distribution

We will consider a receiver loop at a depth of 50 mm oriented in the x direction such that its magnetic moment is parallel to the transmitter plane, as shown in Fig. 1. In [4], the current distribution maximizing the received power through the H-field at the receiver was analytically derived for a multilayer model of tissue. The optimal current distribution $\mathbf{J}$ can be decomposed into J_r and J_θ components that both contribute to the focused H-field. Since the J_θ component tends to incur greater tissue heating, we consider synthesis of only the J_r component.

The magnitude of the optimal J_r distribution is shown in Fig. 1(a). The distribution decreases rapidly with radial distance; beyond a radius of 65 mm, the current is negligible. The phase of J_r is constant along all semicircles and is reversed across the x axis. To simplify the distribution, we observe that most of the energy is concentrated at the maximum located at a radius of about 40 mm. If the current is thresholded, the distribution results in two arcs that are 180° out of phase. Taking the curl of the electric current, the current distribution reduces to two opposing magnetic current paths, as shown in Fig. 1(b).

3. Antenna Design and Feed Network

The slot antenna produces a magnetic current along the opening of the slot. The simplified current distribution can thus be realized by two opposing curved slots with opposite phase. In order to enable power transfer for rotated receiver oriented in the y direction, we introduce an identical slot pair rotated 90°. The design thus consist of two slot pairs, as shown in Fig. 2(a). The slots are designed to operate at about $0.5\lambda_g$ at 2 GHz with a loading FR-4 substrate ($\varepsilon_r = 4.3$), such that the total length is 50 mm. The four slots are excited with equal phase and magnitude by a 4-port feed network placed underneath

the ground plane, as illustrated in Fig. 2(b). The antenna prototype was fabricated on the FR-4 substrate with dimensions 200 mm × 200 mm and a thickness of 1 mm.

3.1 Experimental Results

Fig. 3 shows the reflection coefficient (dB) of the antenna operating at 2 GHz. The simulations were performed by CST MW-Studio. Deviations of the measured results from simulation may be due to inaccuracies in measurement setup compared to the tissue model used in simulation. Fig. 4 shows the experimental setup for the magnetic field measurements. The fabricated transmitter is connected to Agilent E8257D signal generator and faces a receiving small loop antenna of area 4 mm^2 (manufactured by AET, Inc.) placed in a saline solution. The distance between the antenna and the surface of the saline solution is 10 mm. The receiving loop is connected to an Agilent E4407B signal analyzer and is controlled with a 3D positioner. The receive plane magnetic field was measured by separately acquiring the x and y component of the H-field and then computing the magnitude. The saline solution has a dielectric permittivity of $\varepsilon_r = 53$ and loss tangent of 0.25 at 2 GHz.

Fig. 5(a) and 5(b) show the simulated and the measured receive plane magnetic field in air 2 mm below the antenna. The measurement and simulation results at this plane are in agreement; in both cases, the maximum H-field is found on the ends of each slot. The antenna design thus correctly synthesizes the desired magnetic current distribution. The receive plane magnetic field measured in the saline solution 50 mm below the antenna is shown in Fig. 5(c) and 5(d). The half-power focal spot in both simulation and measurement is several mm in radius, which demonstrates H-field focusing.

4. Conclusion

We presented a slot antenna array for power transfer to a miniature implant in tissue. The design is based on curved slot pairs that synthesize a simplified representation of the optimal current distribution found in analysis. An additional slot pair is included to provide efficient power transfer regardless of the horizontal orientation of the implant. The antenna prototype clearly exhibits a focused magnetic field in tissue in both simulation and measurement.

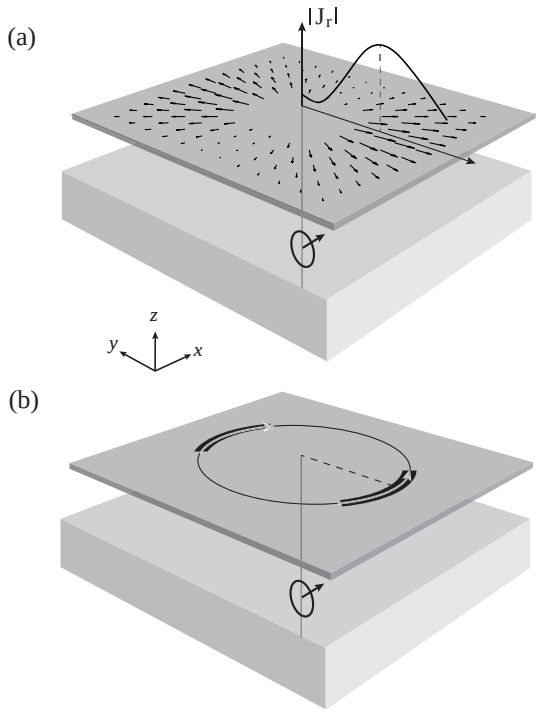

Figure 1: (a) Magnitude of the optimal electric current distribution J_r component and (b) simplified current distribution in terms of magnetic current.

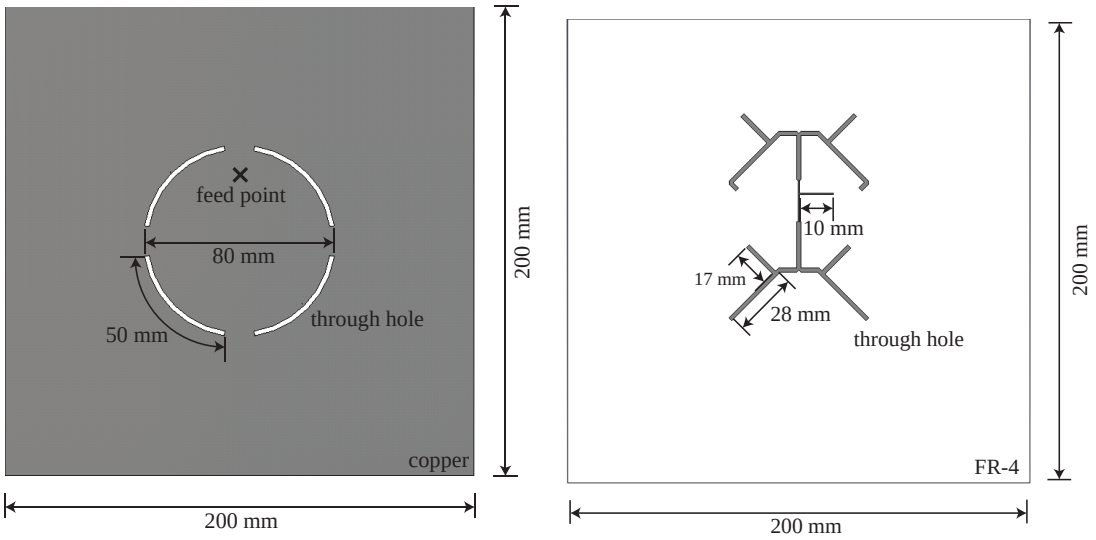

(a) Front side (slot array) (b) Back side (feed network)

Figure 2: Antenna structure.

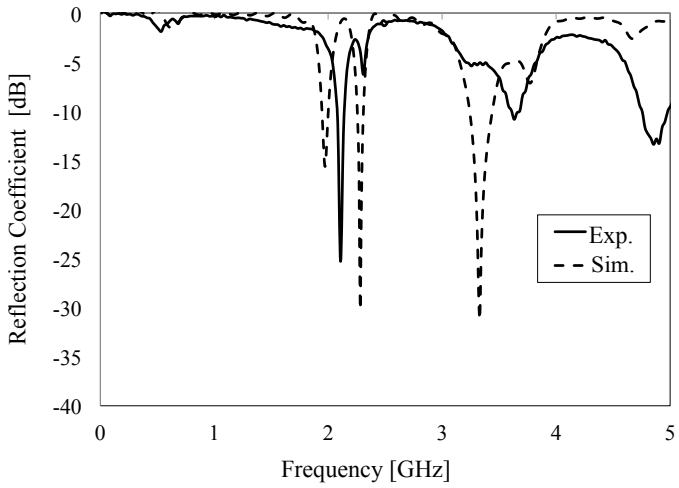

Figure 3: Result of reflection coefficient measurements in air (normalized to 50 Ω).

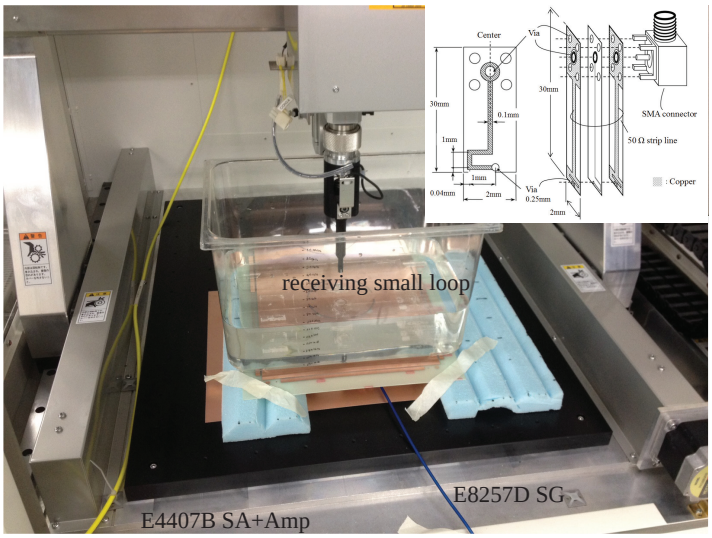

Figure 4: Measurement setup.

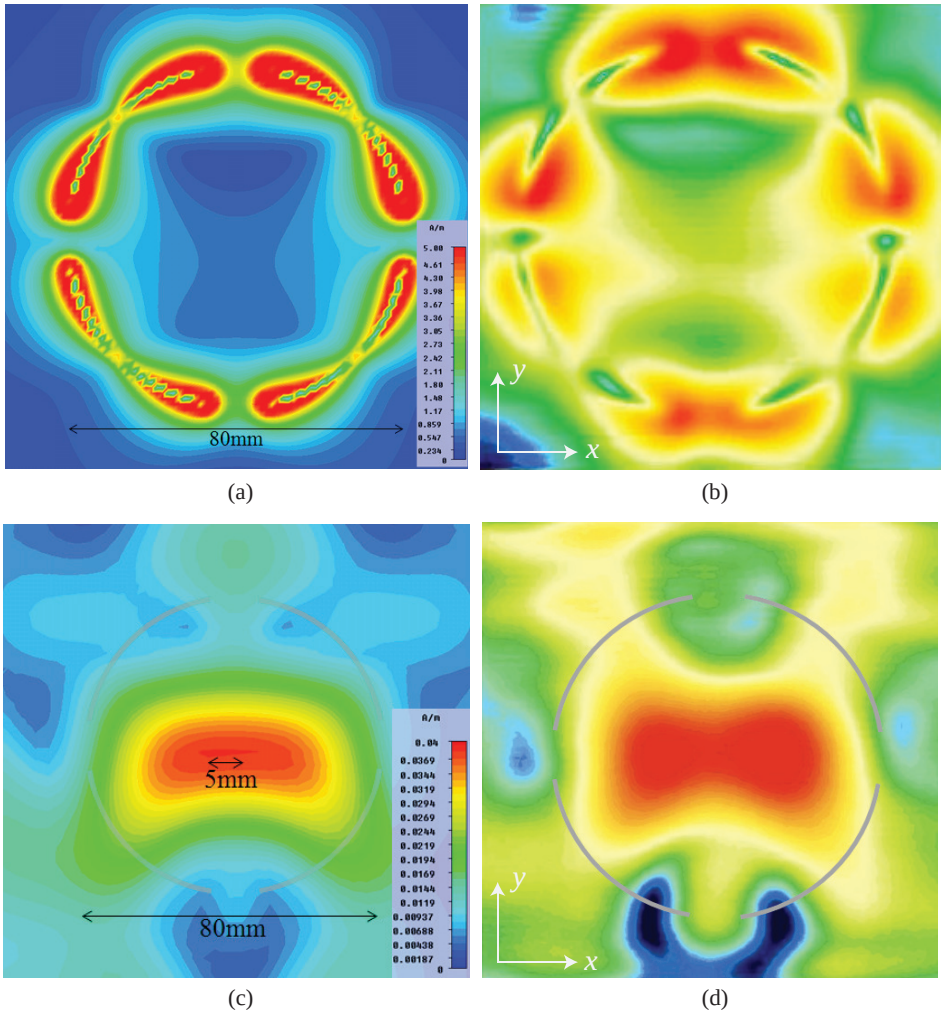

Figure 5: Receive plane magnetic field distribution in air (2 mm below the antenna surface) obtained through (a) simulation and (b) measurement. The magnetic field in saline solution (50 mm deep from the antenna surface) is also shown for (c) simulation and (d) measurement.

References

[1] A. RamRakhyani, S. Mirabbasi, M. Chiao, "Design and optimization of resonance-based efficient wireless power delivery systems for biomedical implants," IEEE Trans. Biomedical Circuits and Systems, vol.5, pp.48-63, Feb. 2011.

[2] A. S. Y. Poon, S. ODriscoll, T. Meng, "Optimal frequency for wireless power transmission into dispersive tissue," IEEE Trans. Antennas and Propagation, vol. 58, pp. 1739-1750, May 2010.

[3] S. Kim, A. S. Y. Poon, "Optimization of source distribution in wireless power transmission for implantable devices," Antennas and Propagation Society International Symposium (APSURSI), pp.1-4, July 2010.

[4] S. Kim, J. S. Ho, A. S. Y. Poon, Wireless power transfer to miniature implants: transmitter optimization, submitted to IEEE Trans. Antennas and Propagation, 2011.